

Faddeev-Hopf knots: Dynamics of linked un-knots

Jarmo Hietarinta

Department of Physics, University of Turku
FIN-20014 Turku, Finland

and

Petri Salo

Helsinki Institute of Physics, P.O. Box 9 (Siltavuorenpenger 20 C)
University of Helsinki, FIN-00014 Helsinki, Finland

August 21, 2018

Abstract

We have studied numerically Faddeev-Hopf knots, which are defined as those unit-vector fields in R^3 that have a nontrivial Hopf charge and minimize Faddeev's Lagrangian. A given initial configuration was allowed to relax into a (local) minimum using the first order dissipative dynamics corresponding to the steepest descent method. A linked combination of two un-knots was seen to relax into different minimum energy configurations depending on their charges and their relative handedness and direction. In order to visualize the results we plot certain gauge-invariant iso-surfaces.

The theory of knots has a long history in mathematics and physics and research on this topic has again become very active, partially due to the possible real world applications (DNA knotting etc). In the late 19th century knots were proposed as models of atoms, and although this idea did motivate the mathematical study of knots, it did not last as a model for physical reality. Now, with the advent of string theory, the possibility of knotted elementary structures has been considered again even in particle physics. In order to give knots a physical meaning one has to give them some physical properties, e.g., thickness and energy. For example, one may assume that there is a charge distribution on the wire and then find its minimum energy configuration [1].

The starting point for the knots discussed in this paper is classical field theory with a unit-vector field defined everywhere in the 3-dimensional space. The unit vector can be considered as a point in S^2 ; furthermore, if at spatial infinity all vectors point to the same direction (lets say to the north pole, i.e., $\mathbf{n} = (0, 0, 1)$) we can compactify R^3 to S^3 and the vector field provides a map $\mathbf{n} : S^3 \rightarrow S^2$. Such maps can be labeled by their Hopf

charge, $\pi_3(S^2) = \mathbb{Z}$. As an example we mention the following map with Hopf charge one:

$$\begin{aligned} n^1 &= \frac{4(2xz - y(x^2 + y^2 + z^2 - 1))}{(1 + x^2 + y^2 + z^2)^2}, \\ n^2 &= \frac{4(2yz + x(x^2 + y^2 + z^2 - 1))}{(1 + x^2 + y^2 + z^2)^2}, \\ n^3 &= 1 - \frac{8(x^2 + y^2)}{(1 + x^2 + y^2 + z^2)^2}. \end{aligned} \tag{1}$$

(It is easy to see that $\mathbf{n} \rightarrow (0, 0, 1)$ as $x^2 + y^2 + z^2 \rightarrow \infty$, as required). A knot can be associated to the vector field by considering how it turns around. In particular, one can look at the pre-image of the south pole $\mathbf{n} = (0, 0, -1)$; normally it is a closed curve which may form a knot. For the vector field (1) the pre-image of the south pole is the ring $z = 0$, $x^2 + y^2 = 1$, justifying the name “un-knot”. Later it will become clear that the curve forming the (un-)knot has also direction and handedness, and the relevant knot theory is therefore that of “framed links” [2]. [An un-knot of charge Q is obtained from (1) if we replace $x \rightarrow \Re[(x + iy)^Q]/r^{Q-1}$, $y \rightarrow \Im[(x + iy)^Q]/r^{Q-1}$, where $r = \sqrt{x^2 + y^2}$.]

In addition to topology we need physics, in particular we need to define an energy for the field configuration. One requirement is that it should not be feasible to minimize energy by scaling the knotted configuration to zero or infinite size. One early proposal was [3] $E = \frac{1}{2} \int [(\partial_\mu \mathbf{n})^2]^{\frac{3}{2}} d^3x$ (μ -sum over 1 to 3), but this does not contain a scale. In [4] Faddeev proposed the Lagrangian

$$L = \frac{1}{2} \int \{ (\partial_\mu \mathbf{n})^2 + g F_{\mu\nu}^2 \} d^3x, \quad F_{\mu\nu} = \epsilon_{abc} n^a \partial_\mu n^b \partial_\nu n^c, \tag{2}$$

as the energy functional. (The topological term can also be written as $F_{\mu\nu}^2 = \frac{1}{2} (\partial_\mu \mathbf{n} \times \partial_\nu \mathbf{n})^2 = \frac{1}{2} [(\partial_\mu \mathbf{n})^2 (\partial_\nu \mathbf{n})^2 - (\partial_\mu \mathbf{n} \cdot \partial_\nu \mathbf{n})^2]$.) What is important here is that there is now a scale defined by the dimensional coupling constant g . Indeed, the derivatives mean that the integrated kinetic term scales under $r \rightarrow \lambda r$ as λ , and the F^2 term as λ^{-1} . Thus a given initial knotted field configuration (e.g. (1)) should evolve (with suitable added dynamics) to a stable minimized configuration of a given size and shape. Vakulenko and Kapitanskii [5] obtained the lower limit (VK bound)

$$E \geq c \sqrt{g} |Q|^{\frac{3}{4}}, \tag{3}$$

for the energy given by (2), here c is some constant, g the coupling constant in (2), and Q the Hopf charge.

The first numerical results with Lagrangian (2) were obtained by Faddeev and Niemi [6, 7] (for popularizations see [8]) and Gladikowski and Hellmund [9]. They studied mainly charge 1 and 2 un-knots, although the possibility of real knots was briefly discussed in [6, 7]. The purpose of this letter is to describe the dynamics of *linked* un-knots. We find that under minimization the linked un-knots can deform to other configurations following the rules applicable to framed links (Kirby moves).

The results of [6, 7] were obtained by a computational method that is different from the one used here. Furthermore, in those papers a rotationally symmetric ansatz was used, because it reduces the computations to the two-dimensional space containing the z axis. However, this reduction also means that stability under rotation-dependent perturbations cannot be probed. It turns out that such effects can be seen already for the charge 3 unknot for which the minimum energy configuration is not rotationally symmetric [10]. Our method is well suited for knots of more complicated topology and we will report some fairly complicated minimization dynamics for linked un-knots. In [6, 7] another simplification was made in handling the unit-vector field. After all, the three components of a unit vector are not independent and one can instead use the two components defined by $w \equiv U + iV = (n^1 + in^2)/(1 + n^3)$. Unfortunately there is a numerical problem in using w instead of \mathbf{n} , due to the fact that the range of U and V is from $-\infty$ to $+\infty$. The singular values are attained along a curve forming the knot, i.e., where $\mathbf{n} = (0, 0, -1)$. It is clear that in a relaxation process it is very expensive to try to move infinities. Indeed, in [6, 7] the infinite inertia of the $w = \infty$ ring was compensated by changing the coupling constants to best fit the virial theorem. The behavior near this infinity ring is also doubtful, because controlling overflow situations may cause unexpected effects.

To avoid the problems mentioned above we decided from the very beginning to put the system on a cubic lattice and use unit-vector fields themselves. Thus, the unknowns were n_{ijk}^α , where i, j, k give the location on the lattice and α the component, $\sum_{\alpha=1}^3 (n_{ijk}^\alpha)^2 = 1$, $\forall i, j, k$. For the kinetic energy term derivatives of \mathbf{n} were discretized on links, that is

$$\int (\partial_\mu \mathbf{n}(x, y, z))^2 d^3r \rightarrow \sum_{i,j,k,\alpha} [(n_{i+1jk}^\alpha - n_{ijk}^\alpha)^2 + (n_{ij+1k}^\alpha - n_{ijk}^\alpha)^2 + (n_{ijk+1}^\alpha - n_{ijk}^\alpha)^2] \delta.$$

For the potential term we discretized $F_{\mu\nu}$ as defined in (2) on the (μ, ν) plaquette. To make it completely symmetric we used in F_{xy} , say,

$$\begin{aligned} n^\alpha &\rightarrow \frac{1}{4}(n_{ijk}^\alpha + n_{i+1jk}^\alpha + n_{i+1j+1k}^\alpha + n_{ij+1k}^\alpha), \\ \partial_x n^\alpha &\rightarrow \frac{1}{2\delta}[(n_{i+1jk}^\alpha - n_{ijk}^\alpha) + (n_{i+1j+1k}^\alpha - n_{ij+1k}^\alpha)], \\ \partial_y n^\alpha &\rightarrow \frac{1}{2\delta}[(n_{ij+1k}^\alpha - n_{ijk}^\alpha) + (n_{i+1j+1k}^\alpha - n_{i+1jk}^\alpha)]. \end{aligned}$$

Minimization of the energy was done using the steepest descent method: $\mathbf{n}_{new} = \mathbf{n}_{old} + \delta t \nabla L$, which corresponds to the dissipative dynamics $\dot{\mathbf{n}} = \nabla L$. This was sometimes accelerated by taking into account also the gradient of the previous step. The expression for the gradient was calculated from the discretized Lagrangian using the symbolic algebra program Reduce. We did not use Lagrange multipliers, but rather renormalized \mathbf{n}_{new} to preserve unit length. On the lattice boundary the vector was fixed to $\mathbf{n} = (0, 0, 1)$. The fact that the system was put into a box with fixed boundaries introduced some boundary pressure. For this reason we cannot exactly attain the prediction of the virial theorem stating that the topological and kinetic energies should be equal.

We did first some calculations on a 50^3 and 100^3 lattices, but it soon became clear that even for un-knots the discretization effects could sometimes change the outcome: If the lattice is too small some neighboring vectors could turn anti-parallel and break the topology. The present computations were done on a 240^3 lattice divided into 4^3 processors on Cray T3E parallel machine. Each round of iteration took about 2 seconds. Typical runs took around 60-70.000 iterations, i.e., 30-40 hours (for charge 1 and 2 linked un-knots). Also, to make sure there were no topology-breakup effects we followed the nearest-neighbor differences of the vectors, in our computations $\max |\mathbf{n} \cdot \mathbf{n}_{nn} - 1|$ was large only at the very beginning and even then the differences never exceeded 0.1 and later were typically 0.02.

It is, in general, hard to visualize vector-fields in three dimensions. Often we associate flow lines to vector fields by imagining how a test particle would move if the vector field would be its velocity field. In the present case, however, this method is not relevant. The point is that there is a global gauge invariance and field lines change in an essential way under such global rotations.

As was said before, the unit vector field provides a map $R^3 \sim S^3 \rightarrow S^2$. We have one fixed direction, that of the vector at infinity ($\mathbf{n} = (0, 0, 1)$), which defines the north pole of S^2 . The unit vector at any other point is defined by its *latitude* and *longitude*. In our illustrations we have chosen to display the pre-image of some latitude circle, that is, the surface where the vector field has a fixed angle with the vacuum direction, i.e., where n^3 has a fixed value.

The longitude is described by colors on the iso-latitude surface. This is suitable because colors are commonly put on a circle anyway: red \rightarrow yellow \rightarrow green \rightarrow blue \rightarrow magenta \rightarrow red¹. The actual position of the 0 meridian is not important, because it is a gauge dependent quantity. The figures were made using the program "funcs" [11] running on a Silicon Graphics O2.

The vector field (1) is not that suitable as an initial configuration for numerical analysis because its kinetic energy density decreases only as r^{-4} as $r \rightarrow \infty$ and therefore the integral itself as r^{-1} . Thus, we introduced some radial squeezing for large r intended to minimize interaction with the box boundaries, and some expansion for small r to decrease the rapid changes at the center. From such a starting configuration a single un-knot relaxed fairly rapidly (in about 30-40.000 iterations) into the minimum configuration. Usually we followed the minimization until the changes in the energy were of the order 10^{-7} per iteration. The same was done for the charge 2 un-knot. In both cases the final configuration seemed to be rotationally symmetric, as can be seen from Figure 1. From these results we infer that for our normalizations the constant c in the VK bound (3) is about 380.

In order to test stability under non-rotational perturbations we took the final result of

¹ Unfortunately the coloring algorithm we used did not completely support the color-circle idea: For example, even if the values 0 and 1 were to stand for the same color, a triangle with corner values 0, 0 and 1 was painted with the color corresponding to the average $1/3$.

an un-knot (with charge 1 or 2), cut it into two semi-tori, separated them by the distance of 20% of the lattice length by repeating the middle configuration, and embedded the new configuration back into the original lattice. The relaxation quickly took this configuration into the original circular form [12].

From Figure 1 one can clearly see that the un-knot has both handedness and direction. The handedness can be determined e.g. by holding the ring and checking with which hand the thumb is aligned along the color boundaries. A right-handed ring (corresponding to (1)) has positive Hopf charge. We can arbitrarily associate a direction to the positive charge un-knot, we use the color direction red \rightarrow yellow \rightarrow green \rightarrow blue \rightarrow magenta \rightarrow red. It turns out that for the left-handed (=negative charge) un-knot we should define the direction by the opposite color sequence.

Our main object was to study the relaxation dynamics of linked un-knots. The first problem was to construct suitable initial configurations. For a single un-knot we could use analytical formulae, but for linked configurations this cannot be as easily done with one formula. Besides, it would be better to use the already relaxed numerical results as starting configurations. We therefore chose a “cut and paste” technique.

Two un-knots each in a box of size L^3 (scaled, if necessary, to the same g value) are immersed into a box of size $(2L)^3$ as described in Figure 2. Assume that the ring of the first un-knot is on the (x, y) -plane and at infinity the vectors point to the positive z -direction. From this single un-knot configuration \mathbf{n} we use the part $0 < x < L, 0 < y < L, \frac{1}{4}L < z < \frac{3}{4}L$. The new configuration \mathbf{N} in the large cube contains, at first, eight pieces defined by \mathbf{n} as follows: (the variable range is always $0 < x < \frac{1}{2}L, 0 < y < \frac{1}{2}L, \frac{1}{4}L < z < \frac{3}{4}L$)

$$\begin{aligned}
\mathbf{N}(x, y + \frac{1}{4}L, z + \frac{1}{2}L) &= \mathbf{n}(x, y, z), \\
\mathbf{N}(x, y + \frac{3}{4}L, z + \frac{1}{2}L) &= \mathbf{n}(x, \frac{1}{2}L, z), \\
\mathbf{N}(x, y + \frac{5}{4}L, z + \frac{1}{2}L) &= \mathbf{n}(x, y + \frac{1}{2}L, z), \\
\mathbf{N}(x + \frac{1}{2}L, y + \frac{5}{4}L, z + \frac{1}{2}L) &= \mathbf{n}(\frac{1}{2}L, y + \frac{1}{2}L, z), \\
\mathbf{N}(x + L, y + \frac{5}{4}L, z + \frac{1}{2}L) &= \mathbf{n}(x + \frac{1}{2}L, y + \frac{1}{2}L, z), \\
\mathbf{N}(x + L, y + \frac{3}{4}L, z + \frac{1}{2}L) &= \mathbf{n}(x + \frac{1}{2}L, \frac{1}{2}L, z), \\
\mathbf{N}(x + L, y + \frac{1}{4}L, z + \frac{1}{2}L) &= \mathbf{n}(x + \frac{1}{2}L, y, z), \\
\mathbf{N}(x + \frac{1}{2}L, y + \frac{1}{4}L, z + \frac{1}{2}L) &= \mathbf{n}(\frac{1}{2}L, y, z).
\end{aligned}$$

The other un-knot is inserted similarly, but first it must be turned so that it lies in the (x, z) -plane, by $\mathbf{n}'(x, y, z) = \mathbf{n}(x, z, L - y)$. (Note that this only moves the vectors without changing their directions.) The remaining empty sub-blocks are filled with vectors pointing up. The above construction makes sense only if there are no discontinuities at the boundaries. In particular, it is necessary that also at the center of the initial un-knot the vector points up: $\mathbf{n}(\frac{1}{2}L, \frac{1}{2}L, z) = (0, 0, 1)$.

In Figure 3 we show the initial and final results for some linked configurations[12]. On the left is the initial configuration (constructed in the way described) after a few iterations. In each case the ring on the (x, y) -plane (on the left side of the linked combination) is the

same, it is right-handed with Hopf charge $+1$ and has counterclockwise color direction if we look from the positive z direction. In the top two figures the part that lies in the (x, z) -plane also has charge $+1$, but the parts are linked differently, in (a) the linking is such that the color direction is down through the un-knot in the (x, y) plane and then the linking number is $+2$, for (b) it goes up and the linking number is -2 , c.f., Figure 4. For the two lower figures the other un-knot is left-handed (charge -1) and when we recall the different definitions of direction mentioned above, the direction in (c) is from above and for (d) from below.

The total charge of the linked configuration is the sum of the charges of the initial un-knots and ± 2 for linking, and it is this total charge that is conserved under minimization. For (b) the sum is zero and indeed the final configuration is on its way to the vacuum where all vectors point up. For (c) the sum is $+2$ and for (d) -2 which are the charges of the final un-knots. It should be noted that we did not continue the minimization too long after the form of the final configuration became clear, because it was already known that deformed charge 2 un-knots return to their original shape. For (a) the sum is $+4$ and the configuration seems to be stable. The total energy of this configuration is not too far from what is predicted by the VK bound (within 10%). A plot of energy vs. iteration step is given in Figure 5.

The form of the final state depends on the relative color positions of the two un-knots. This is illustrated in Figure 6. The two final configurations are different because the color orientations of the initial un-knots in the (x, z) -plane were different, corresponding to a 90° rotation around the y axis [12]. The initial color difference has not changed much in the minimization, instead we see that the un-knots are twisted differently.

We also studied the dynamics related to the four ways of combining un-knots of charge ± 2 [12]. The results agree with the addition rule, their energy plots have been included in Figure 5. Again the $2 + 2 + 2$ configuration seems to be stable, when we stopped minimization its energy was within 7% of the VK bound.

It should be emphasized that the minimization dynamics represents a smooth deformation of the initial configuration. One way to explain the observed deformations is to describe the configurations in terms of framed links and then to deform them using Kirby moves[2], the details will be discussed elsewhere.

Recently Battye and Sutcliffe observed that higher charge un-knots sometimes deform into more knotted but lower energy configurations [10]. They found, e.g., that a perturbed charge 6 un-knot deformed into the linked combination $2 + 2 + 2$ discussed above. For charge 4 they found a strongly deformed un-knot and it would be interesting to check whether its final state energy really is less than our $1 + 1 + 2$ configuration. Furthermore, they found that the charge 7 un-knot deformed into a trefoil. In order to test whether a trefoil is also obtained from other initial configurations with total charge 7 we constructed a linked combination of charge $+4$ and $+5$ un-knots with linking number -2 . The initial state quickly deformed into a wiggled charge 7 un-knot which then more slowly deformed into a trefoil. On the other hand, the combination $2 + 3 + 2$ remained stable and relaxed

to equally low energies (within 5%).

Our results show that the set of minimum energy configurations of Faddeev-Hopf knots is very rich, and the minimization can take a very complicated route. It would now be very interesting to characterize further the topological properties of these types of knotted configurations. In particular, it would be useful to know which configurations of the same Hopf charge can be smoothly deformed to each other, and whether in such cases there exists a deformation sequence where energy always decreases. In any case we know now that the associated knot theory must take into account the handedness and direction of the curve forming the knot.

Acknowledgments

We would like to thank L. Faddeev, A. Niemi, P. Sutcliffe and W. Zakrzewski for discussions and M. Gröhn for help in the visualization aspects of this work. We are grateful to the Center for Scientific Computing, Espoo, for computer time in the Cray T3E parallel machine, where most of the computations reported here were made.

References

- [1] J.K. Simon, Energy functions for polygonal knots, *J. Knot Theory and its Ramifications* **3**, 299-320 (1994).
- [2] L. Faddeev, private communication.
- [3] D.A. Nicole, *J. Phys. G: Nucl. Phys.* **4**, 1363 (1978).
- [4] L. Faddeev, IAS Print 75-QS70 (1975); L. Faddeev, *Einstein and Several Contemporary Tendencies in the Theory of Elementary Particles* in “Relativity, Quanta, and Cosmology, Vol.1”, M. Pantaleo and F. De Finis, eds., pp. 247-266 (1979), reprinted in L. Faddeev, “40 years in mathematical physics”, pp. 441-461 (World Scientific, 1995).
- [5] A.F. Vakulenko and L.V. Kapitanskii, *Sov. Phys. Dokl.* **24**, 433 (1979).
- [6] L. Faddeev and A. Niemi, *Nature* **387**, 1 May, 58, (1997), [hep-th/9610193](#).
- [7] L. Faddeev and A. Niemi, [hep-th/9705176](#).
- [8] W. Perkins, *Nature*, **387**, 1 May, 19 (1997); *New Scientist*, 27 Sept, 30 (1997).
- [9] J. Gladikowski and M. Hellmund, *Phys. Rev. D* **56**, 5194 (1997), [hep-th/9609035](#)
- [10] R. Battye and P. Sutcliffe, *Solitonic Strings and Knots*, preprint; *To be or knot to be* [hep-th/9808129](#).
- [11] Developed by J. Ruokolainen, Center for Scientific Computing, Espoo, Finland. <http://www.csc.fi/jpr/funcs/funcs.html>
- [12] Relevant video animation can be seen at <http://www.utu.fi/~hietarin/knots>

Figure captions

Figure 1. The final configurations for charge 1 and 2 un-knots. The displayed iso-surfaces correspond to the equator, i.e., have $n^3 = 0$.

Figure 2. Constructing a linked combination from separate un-knots by cut and paste. The vector field has the vacuum direction at the boundaries marked by thick lines.

Figure 3. Initial and final configurations for the four ways of linking a charge +1 un-knot with a charge ± 1 un-knot. On the left-hand column we have the initial configuration, at the center some intermediate state, and on the right the “final” state (iso-latitude surfaces $n^3 = -0.5$). The charges and linking numbers are (a) $1 + 1 + 2$, (b) $1 + 1 - 2$, (c) $1 - 1 + 2$, (d) $1 - 1 - 2$.

Figure 4. Rules for linking number from color direction.

Figure 5. Energy as a function of the iteration step for various linked combinations. A: $1 + 1 + 2$, B: $1 + 1 - 2$, C: $1 - 1 + 2$, D: $1 - 1 - 2$, E: $2 + 2 + 2$, F: $2 + 2 - 2$, G: $2 - 2 + 2$, H: $2 - 2 - 2$.

Figure 6. Two final states for the $1 + 1 + 2$ configuration. The initial states had different color orientation in the un-knot on the (x, z) plane (iso-latitude surfaces $n^3 = -0.8$).

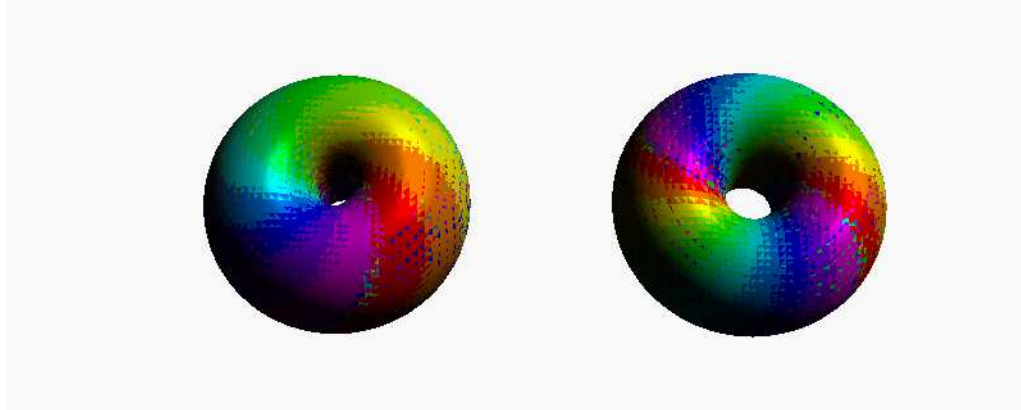


Figure 1: The final configurations for charge 1 and 2 un-knots. The displayed iso-surfaces correspond to the equator, i.e., have $n^3 = 0$.

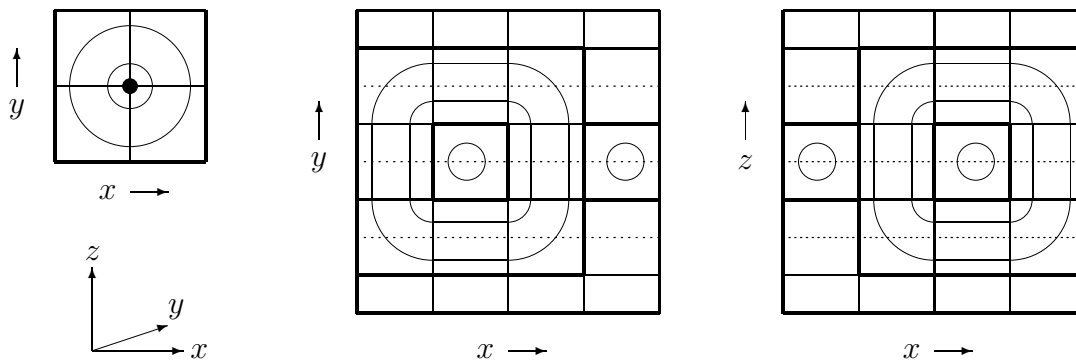


Figure 2: Constructing a linked combination from separate un-knots by cut and paste. The vector field has the vacuum direction at the boundaries marked by thick lines.

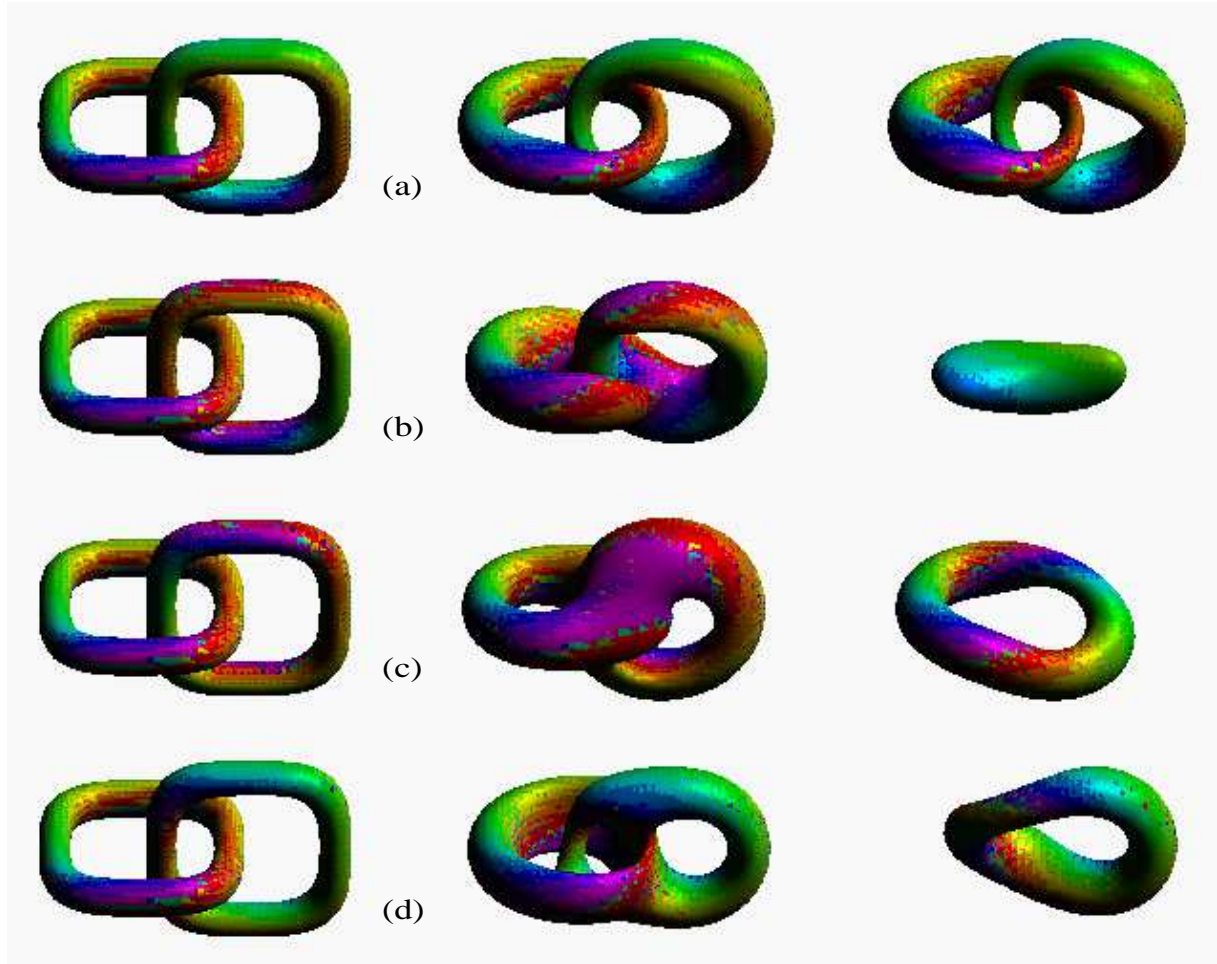
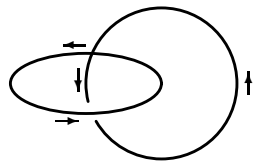
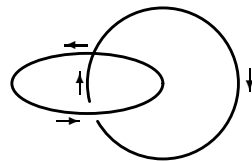


Figure 3: Initial and final configurations for the four ways of linking a charge +1 un-knot with a charge ± 1 un-knot. On the left-hand column we have the initial configuration, at the center some intermediate state, and on the right the “final” state (iso-latitude surfaces $n^3 = -0.5$). The charges and linking numbers are (a) $1 + 1 + 2$, (b) $1 + 1 - 2$, (c) $1 - 1 + 2$, (d) $1 - 1 - 2$.



Linking number +2.



Linking number -2.

Figure 4: Rules for linking number from color direction.

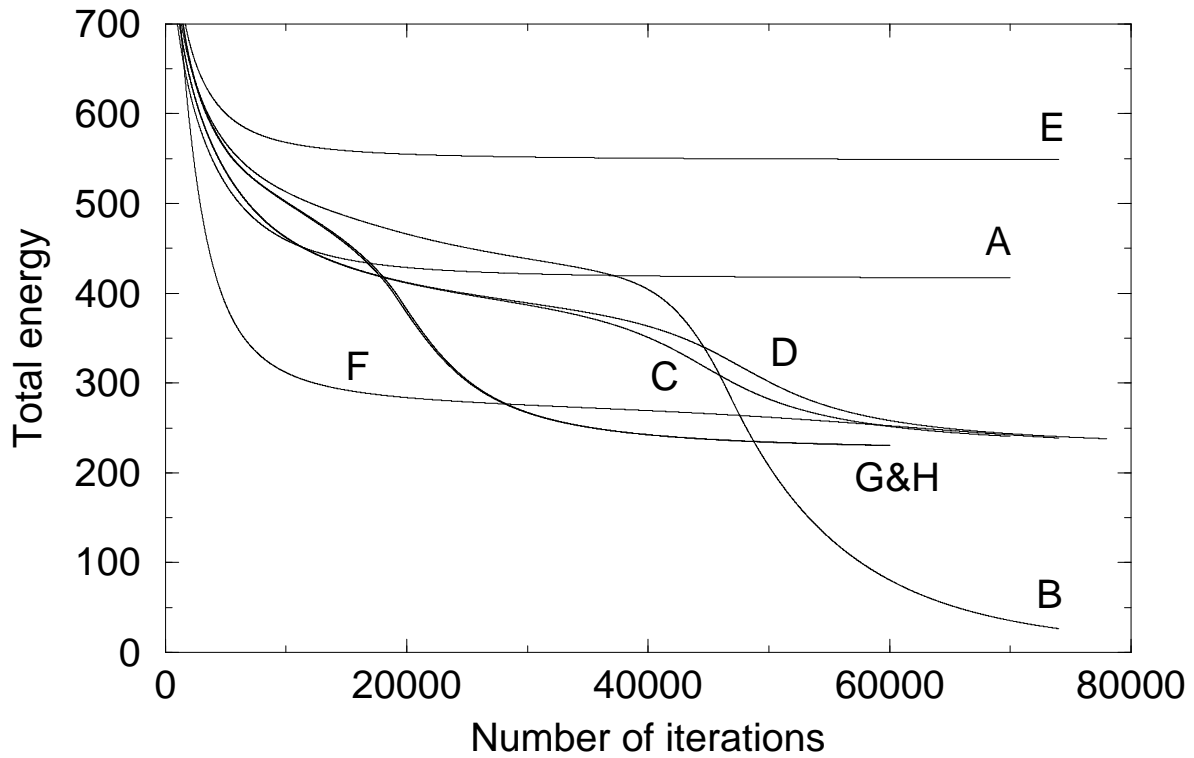


Figure 5: Energy as a function of the iteration step for various linked combinations. A: $1 + 1 + 2$, B: $1 + 1 - 2$, C: $1 - 1 + 2$, D: $1 - 1 - 2$, E: $2 + 2 + 2$, F: $2 + 2 - 2$, G: $2 - 2 + 2$, H: $2 - 2 - 2$.

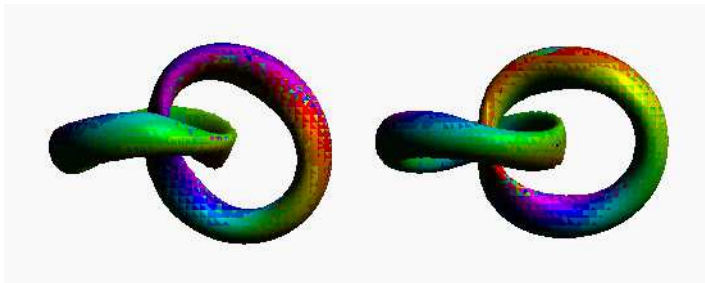


Figure 6: Two final states for the $1 + 1 + 2$ configuration. The initial states had different color orientation in the un-knot on the (x, z) plane (iso-latitude surfaces $n^3 = -0.8$).